ELSEVIER

Thermochimica Acta 280/281 (1996) 101–126

thermochimica acta

Transient nucleation[1]

P. Demo *, Z. Kožíšek

Institute of Physics, Academy of Sciences of the Czech Republic, Na Slovance 2, 180 40 Praha 8, Czech Republic

Abstract

Nucleation plays an important role in phase transformation processes. This review represents an attempt towards a synoptical description of this phenomenon at the kinetic level (including thermodynamical considerations) and summarizes our most interesting results connected with this theme for both single component and binary systems.

Keywords: Crystallization; Kinetics; Model; Nucleation; Phase transformation

1. Introduction

The theory of crystal growth, one of the bases of modern high technologies, deals with the problems of how to model processes taking place during production of a new phase of required physico-chemical properties. It is aimed at understanding what happens when fluid (gas, solution, melt) becomes solid (or liquid) and how to govern this transformation by limited conditions adjustable and controllable from the outside.

Nucleation may be understood to be an initial stage of the process leading to the formation of clusters (embryos) of new phase (solid or liquid) within the metastable parent phase (undercooled melt, supersaturated fluid). Indeed, due to sufficiently large fluctuations, intrinsic (thermal), or artificially induced from the outside, small portions of the product phase may appear. In such a way, homogeneous nucleation occurs at random sites in the bulk of the original phase whilst heterogeneous nucleation takes place at preferrential sites, such as impurities, defects, substrates, and crucible walls.

---

* Corresponding author

[1] Dedicated to Professor Hiroshi Suga.

SSDI 0040-6031(95)02638-X

Although the model of the nucleation process was known in the 1930s and considerable effort has been directed towards a deeper understanding of this problem, a number of questions remains, until now, unanswered (for more details see, e.g. Refs. [1–4]). Essentially, they can be divided into three groups:

(i) Adequate definition of appropriate thermodynamical quantities expressing (local) equilibrium properties of the nucleating system, e.g. the Gibbs energy required to form a cluster consisting of n molecules or atoms, the surface energy between a cluster and its ambient phase, etc;
(ii) Proper modeling of the kinetic parameters entering the nucleation equation; in particular, the transition probability that a particle joins to a cluster of size n (sometimes called the "rate constant");
(iii) Solution of the nucleation equation and determination of important characteristics of the nucleation process itself (such as nucleation rate, number of nuclei within the system at a given time, time lag, etc.).

In this article, we deal with the problems of homogeneous nucleation occurring under constant, or variable temperature regimes in single and also in binary systems. We have solved the nucleation (Zeldovich–Frenkel) equation numerically and also obtained an approximate analytical solution, which seems to be more transparent and applicable, especially in engineering applications. Results are compared with solutions of other authors and also with available experimental data.

2. Thermodynamical aspects of nucleation

Consider a metastable mother phase consisting of N molecules or atoms (monomers) maintained at temperature T. (Usually, the total number of monomers N is assumed to be constant.) As stated above, as a consequence of thermal fluctuations, variously sized clusters are formed within the bulk of the parent phase. We assume that the principle of local (thermodynamic) equilibrium is satisfied, i.e. although the system is in non-equilibrium state en bloc, we assume that equilibrium between newly formed clusters and ambient phase is already established. Then, following simple thermodynamics, the Gibbs free energy (alternatively, the excess Gibbs energy) $\Delta G(n)$ required to form a cluster of n monomers is given by the difference between the appropriate Gibbs energies corresponding to the product (G_P) and initial (G_I) phases, e.g. Ref. [5]

$$\Delta G(n) = G_P - G_I \tag{1}$$

An alternative formula to relation (1) is [6]

$$\Delta G(n) = \Delta G_V(n) + \Delta G_S(n) \tag{2}$$

where ΔG_V represents the volume contribution to the formation of an embryo, whilst ΔG_S is connected with the free energy consumed to creation of the interface between the cluster and the parent phase. The concrete form of $\Delta G(n)$ depends on the kind of material under consideration (single or multicomponent system, ideal gas, regular solution, etc.).

Newly-formed clusters are unstable below a certain critical size n^*, whose value may be determined from the extremum condition

$$\frac{\partial \Delta G(n)}{\partial n} = 0 \tag{3}$$

in the case of single component system, and

$$\frac{\partial \Delta G(n_A, n_B, \ldots)}{\partial n_i} = 0 \quad i = A, B, \ldots \tag{4}$$

for multi-component system, where $n_A, n_B, \ldots$ represent the numbers of molecules (atoms) of A, B, ... components within the cluster. Depending on the ratio of the surface (ΔG_S) and volume (ΔG_V) contributions to the Gibbs energy, the critical cluster typically contains from a few tens of molecules, for example, in glassy melts, to several thousands of monomers, in the case of cloud formation. Above the critical size n^*, the clusters become nuclei and tend to grow.

2.1. Single-component system

In this case, relationship (1) may be rewritten as

$$\Delta G(n) = -n(\mu_I - \mu_P) + [\mathcal{G}(n) - n\mu_P] \tag{5}$$

where μ_P is the chemical potential (per particle) of particles contained within a cluster, μ_I stands for the chemical potential of the initial phase and $\mathcal{G}(n)$ denotes the Gibbs free energy corresponding to the n-molecular cluster en bloc.

The term $\Delta\mu = \mu_I - \mu_P$ on the r.h.s. of relation (5) represents the thermodynamic driving force of the nucleation process (supersaturation, undercooling) and is closely connected with the rate of departure of the system from the equilibrium state (in which, of course, $\Delta\mu = 0$). If the nucleation occurs in a supersaturated vapor, then $\Delta\mu \sim \ln S$, where S stands for supersaturation ratio [1]. In the case of the melts, the following formulae are frequently used

$$\Delta\mu = \frac{\Delta h \Delta T}{N_A T_E} \tag{6}$$

or

$$\Delta\mu = \frac{\Delta h \Delta T}{N_A T_E} \frac{T}{T_E} \tag{7}$$

Here, Δh denotes the heat of fusion, N_A is Avogadro's number, T_E represents the melting temperature, and $\Delta T = T_E - T$ is undercooling. (The above relationships can be readily derived by expanding, as usual, $\Delta\mu$ in the Taylor series at the melting temperature T_E; for details see, e.g. Refs. [7–11].)

The second term on the r.h.s. of formula (5) reflects the creation of a new interface

$$\mathcal{G}(n) - n\mu_P = S_n \sigma \tag{8}$$

where $S_n = \gamma n^{2/3}$ denotes the cluster surface, σ is the interfacial energy, and the so-called form factor γ characterizes the geometry of the cluster. Frequently, spherical clusters are considered (for which the ratio of surface and volume contributions corresponds to a minimum of ΔG). In this case, $\gamma = (36\pi)^{1/3}\Omega^{2/3}$ ($\Omega = N_A/V_M$ is molecular volume and V_M denotes the molar volume), or, alternatively, $\gamma = 4\pi r_0^2$ (r_0 being the radius of the monomer).

Taking into account the above relationships, one can express the Gibbs free energy as follows

$$\Delta G(n) = -n\Delta\mu + \gamma\sigma n^{2/3} \tag{9}$$

Applying extremum condition (3), we get for the critical size

$$n^* = \left(\frac{2\gamma\sigma}{3\Delta\mu}\right)^3 \tag{10}$$

With a properly defined quantity $\Delta\mu$, the above expressions (9) and (10) are valid for both the vapor→liquid transition and the liquid→solid transformation in single-component systems. The dependency of the Gibbs free energy on the cluster size for two different values of $\Delta\mu$ is shown in Fig. 1.

2.2. Binary system

This situation is more complicated because of an additional variable, i.e. composition. Let n_A (n_B) be the number of molecules of component A (B) involved in a cluster. Evidently, $n = n_A + n_B$. Then the work of formation of a cluster of size n is given by (see,

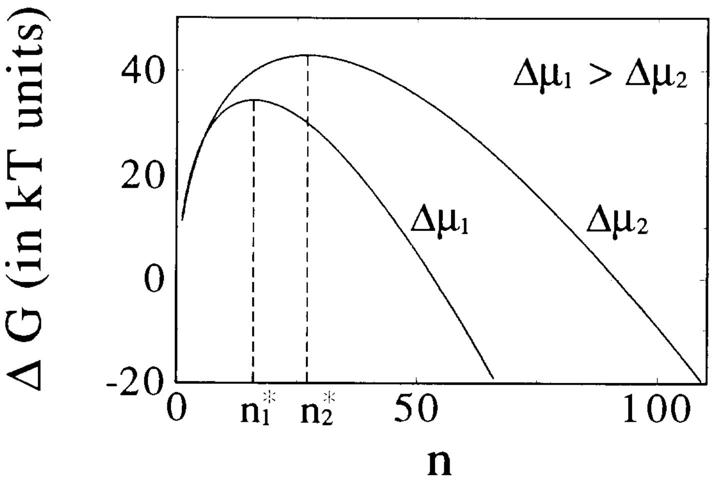

Fig. 1. Schematic dependence of the Gibbs free energy ΔG of a single-component system on the cluster size n for two different values of the difference in chemical potential $\Delta\mu$.

e.g., Refs. [12–14])

$$\Delta G(n_A, n_B) = -n_A kT \ln\left(\frac{a_A n}{n_A}\right) - n_B kT \ln\left(\frac{a_B n}{n_B}\right) + \gamma\sigma n^{2/3} \tag{11}$$

in the case of a vapor–liquid transition, and

$$\Delta G(n_A, n_B) = -n_A \Delta\mu_A^0 - n_B \Delta\mu_B^0 - kT\left[n_A \ln(1 - X_B^L) + n_B \ln X_B^L + \ln\left(\frac{n!}{n_A! n_B!}\right)\right] + \gamma\sigma n^{2/3} \tag{12}$$

for a liquid (melt)–solid transformation. Above, $a_i = P_i/P_i^0$ ($i = $ A, B) is the activity of the ith component (P_i denotes partial and P_i^0 saturation pressures), $\Delta\mu_i^0$ ($i = $ A, B) corresponds to the difference in chemical potentials of the pure components, k is the Boltzmann constant, and X_B^L is the initial mole fraction of component B in the liquid. Nevertheless, the aforementioned relationships hold for ideal systems (vapor, liquid) and become more complex for real materials, e.g. regular solutions, real melts, etc. Appropriate free energies can be derived within the framework of statistical thermodynamics.

Using expression (11) and taking into account conditions (4), the so-called saddle point (n_A^*, n_B^*) on the free energy surface $\Delta G(n_A, n_B)$ can be computed to be

$$n_A^* = \left(\frac{a_A}{a_A + a_B}\right)\left[\frac{2\gamma\sigma}{3kT \ln(a_A + a_B)}\right]^3 \tag{13}$$

and

$$n_B^* = \left(\frac{a_B}{a_A + a_B}\right)\left[\frac{2\gamma\sigma}{3kT \ln(a_A + a_B)}\right]^3 \tag{14}$$

from which the total critical size is obtained

$$n^* = n_A^* + n_B^* = \left[\frac{2\gamma\sigma}{3kT \ln(a_A + a_B)}\right]^3 \tag{15}$$

After tedious calculations, similar formulae may also be derived for the liquid–solid transformation. Supposing that interfacial energy does not depend on concentration, one gets

$$n_A^* = n_B^* \left(\frac{1 - X_B^L}{X_B^L}\right) \exp\left(\frac{\Delta\mu_A^0 - \Delta\mu_B^0}{kT}\right) \tag{16}$$

$$n_B^* = \left(\frac{2\gamma\sigma}{3\alpha}\right)^3 \tag{17}$$

where

$$\alpha = \left[\left(\frac{1 - X_B^L}{X_B^L}\right) \exp\left(\frac{\Delta\mu_A^0 - \Delta\mu_B^0}{kT}\right) + 1\right]^{1/3} \times \left\{kT \ln\left[1 + X_B^L\left(\exp\left(\frac{\Delta\mu_B^0 - \Delta\mu_A^0}{kT}\right) - 1\right)\right] + \Delta\mu_A^0\right\} \tag{18}$$

and the thermodynamic driving force (see Eq. (6)) takes the form

$$\Delta\mu^0_{\mathrm{A,B}} = \frac{\Delta h^0_{\mathrm{A,B}}(T^0_{\mathrm{A,B}} - T)}{T^0_{\mathrm{A,B}}} \tag{19}$$

Above, $\Delta h^0_{\mathrm{A,B}}$ denote the heats of fusion and $T^0_{\mathrm{A,B}}$ are the melting temperatures of pure components A, B. These expressions may be rewritten in terms of new variables, concentration $C = n_{\mathrm{B}}/n$ and cluster size $n = n_{\mathrm{A}} + n_{\mathrm{B}}$. In Fig. 2, the Gibbs free energy as a function of n_{A} and n_{B} is depicted for the case of a liquid–solid model system.

To complete this section, it should be pointed out, however, that there are several approaches which differ from this so-called "capillarity approximation" procedure presented above and allow determination of the free energy of cluster by alternative methods. (For instance, utilizing the order parameter theory of freezing; for more details see, e.g. Ref. [15].)

3. Nucleation kinetics

3.1. General aspects

It is quite clear that the modeling of a transient, i.e. time dependent, nucleation process remains beyond the scope of standard equilibrium thermodynamics and the problem has to be treated in another way. In principle, two complementary methods may be applied. The first is based on purely numerical calculations (so-called "numerical experiments"); in particular, Monte Carlo simulations, or molecular dynamics are frequently used. Alternatively, a physically more transparent approach seems to be the description of transient nucleation at the physical kinetics level.

Within the framework of such an approach, it is assumed that the dominant role of cluster formation is the attachment (detachment) of single particles (atoms, molecules, ions) to (from) the cluster surface. This stepwise kinetic process may be represented schematically in the case of a single-component system as

$$\begin{tikzcd}
(n-1) \arrow[r, shift left, "k^+_{n-1}"] & (n) \arrow[l, shift left, "k^-_n"] \arrow[r, shift left, "k^+_n"] & (n+1) \arrow[l, shift left, "k^-_{n+1}"]
\end{tikzcd}$$

Or more chemically, e.g. Ref. [1]

$$\mathrm{A}(n) + \mathrm{A}(1) \underset{k^-(n+1)}{\overset{k^-(n)}{\rightleftarrows}} \mathrm{A}(n+1) \tag{20}$$

where A(n) is the cluster consisting of n particles, A(1) stands for the single molecule (monomer) and the symbols $k^\pm$ denote the appropriate transition probabilities (transient frequencies) that a single particle joins (+) (or evaporates (−)) to (form) a cluster of given size per unit time. Other types of transitions, such as, for instance

$$\mathrm{A}(n) + \mathrm{A}(l) \underset{k^-}{\overset{k^+}{\rightleftarrows}} \mathrm{A}(n+l), \quad \text{for } n > 1, l > 1 \tag{21}$$

are usually considered to be negligible.

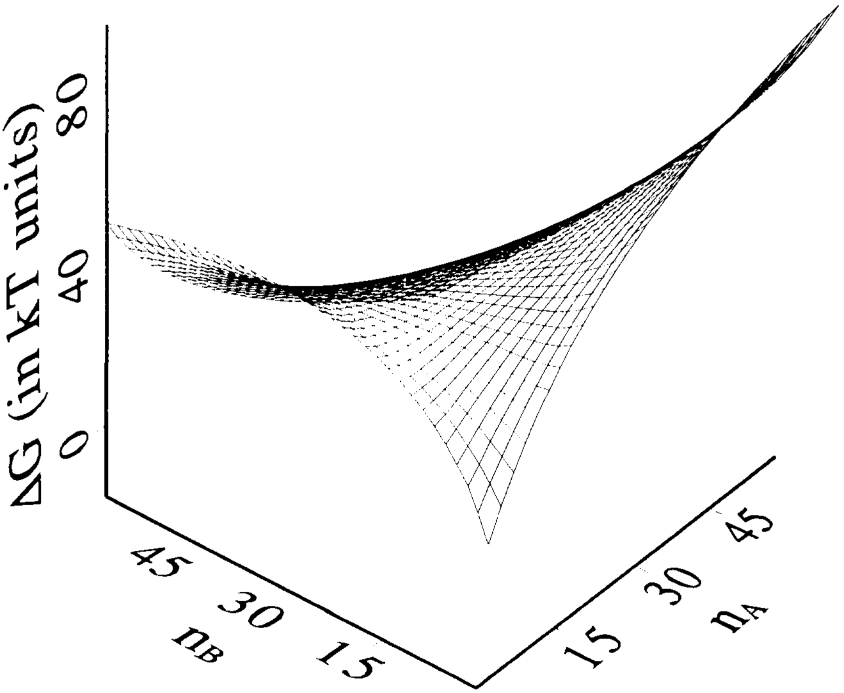

Fig. 2. Schematic dependence of the Gibbs free energy ΔG of a binary model melt on the number of molecules of $A(n_A)$, and $B(n_B)$, components.

For the binary system, the reaction scheme takes the form

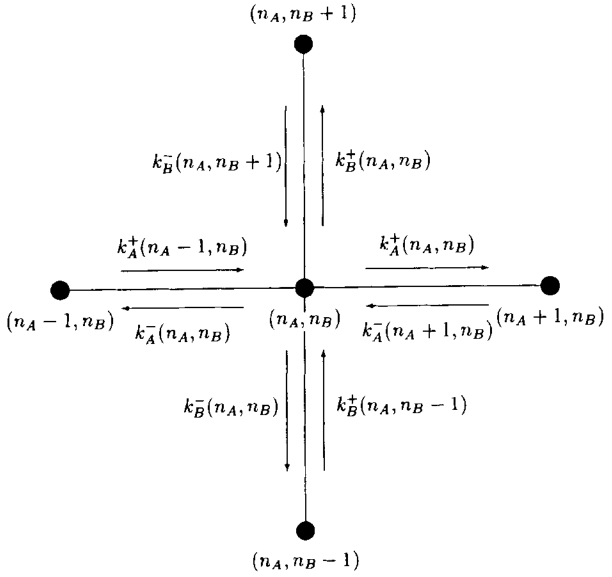

or

$$\mathrm{A}(n_\mathrm{A}, n_\mathrm{B}) + \mathrm{A}(1,0) \underset{k_\mathrm{A}(n_\mathrm{A}+1, n_\mathrm{B})}{\overset{k_\mathrm{A}^+(n_\mathrm{A}, n_\mathrm{B})}{\rightleftharpoons}} \mathrm{A}(n_\mathrm{A}+1, n_\mathrm{B}) \tag{22}$$

$$\mathrm{A}(n_\mathrm{A}, n_\mathrm{B}) + \mathrm{A}(0,1) \underset{k_\mathrm{B}^-(n_\mathrm{A}, n_\mathrm{B}+1)}{\overset{k_\mathrm{B}^+(n_\mathrm{A}, n_\mathrm{B})}{\rightleftharpoons}} \mathrm{A}(n_\mathrm{A}, n_\mathrm{B}+1) \tag{23}$$

Above, $\mathrm{A}(n_\mathrm{A}, n_\mathrm{B})$ is the cluster containing n_A and n_B monomers of A and B and $k^{\pm}_{\mathrm{A,B}}, i = \mathrm{A, B}$ represent the appropriate transition probabilities. As will be seen below, the transition probabilities depend, in general, on the temperature, cluster size $n(= n_\mathrm{A} + n_\mathrm{B})$ and other parameters. (This is why, in our opinion, the generally used term "rate **constants**" is incorrect.)

3.2. *Transient frequencies*

As was already mentioned, the rates $k^{\pm}$ at which monomers condense on (or evaporate from) the cluster of a given size n play an important role in the nucleation model. Concrete forms of these transient frequencies can be derived using the methods of kinetic theory and depend both on the kind of material under consideration and also on the nature of the phase transformation. In particular, two different situations and two varying systems are analysed separately below: condensation, or solidification, in single-component and in binary systems.

3.2.1. *Vapor–liquid transition*

We assume that the speeds of monomers are distributed according to the Maxwell–Boltzmann law. Consequently, the mean number of particles impinging on the unit surface of $n$mer per unit time from the vapor side is readily determined to be [16]

$$v = \frac{N_\mathrm{A}}{V_\mathrm{M}}\sqrt{\frac{kT}{2\pi m}} = \frac{P}{\sqrt{2\pi mkT}} \tag{24}$$

where T is temperature, k denotes the Boltzmann constant, N_A is the Avogadro number, V_M represents molar volume, m is the mass of a single molecule and P is the actual pressure of the vapor. The attachment frequency $k^{\pm}(n)$ then can be expressed as

$$k^+(n) = S_n v = \gamma n^{2/3} v \tag{25}$$

for single-component vapor, and

$$k_i^+(n_\mathrm{A}, n_\mathrm{B}) = S_n v = \gamma(n_\mathrm{A} + n_\mathrm{B})^{2/3} v_i, \quad i = \mathrm{A, B} \tag{26}$$

for a binary system, where S_n denotes the cluster surface. Above, γ is the form-factor and the quantity v_i is defined to be

$$v_i = \frac{P_i}{\sqrt{2\pi m_i kT}}, \quad i = \mathrm{A, B} \tag{27}$$

where P_i corresponds to the partial pressure of the ith component with the mass m_i.

The detachment frequencies $k^-(n)$, and $k_i^-(n_A, n_B)$ of the reverse process, i.e. evaporation, are determinable by the use of detailed balance conditions

$$k^+(n)F_0(n) = k^-(n+1)F_0(n+1) \tag{28}$$

for a single-component system, and

$$k_A^+(n_A, n_B)F^0(n_A, n_B) = k_A^-(n_A+1, n_B)F^0(n_A+1, n_B) \tag{29}$$

$$k_B^+(n_A, n_B)F^0(n_A, n_B) = k_B^-(n_A, n_B+1)F^0(n_A, n_B+1) \tag{30}$$

in the case of binary vapor. Appropriate equilibrium distribution functions are given successively as

$$F_0(n) = N\exp\left[-\frac{\Delta G(n)}{kT}\right] \tag{31}$$

and

$$F_0(n_A, n_B) = (N_A^0 + N_B^0)\exp\left[-\frac{\Delta G(n_A, n_B)}{kT}\right] \tag{32}$$

Here $N_A^0(N_B^0)$ is the number of monomers of the A(B) component, N is the total number of "single" monomers and the Gibbs energies $\Delta G(n)$ and $\Delta G(n_A, n_B)$ are represented by relationships (9) and (11).

3.2.2. *Liquid–solid transformation*

In a single-component liquid, the transient frequency $k^+(n)$ can be expressed as follows [17, 18]

$$k^+(n) = S_n\omega\exp\left(-\frac{q[\Delta G(n+1) - \Delta G(n)]}{kT}\right) \tag{33}$$

where

$$q = \frac{1}{2}[1 + \operatorname{sign}[\Delta G(n+1) - \Delta G(n)]] \tag{34}$$

In fact, Eq. (33) simply states that the clusters are unstable below the critical size and tend to shrink, whereas clusters grow for $n \geq n^*$. Above, $\Delta G(n)$ is given by Eq. (9) and the quantity ω is defined as

$$\omega = \rho_S\left(\frac{kT}{h}\right)\exp\left(-\frac{E}{kT}\right) \tag{35}$$

where kT/h is the frequency of the temperature oscillations of the molecules (atoms) and

$$\rho_S \approx a_0 n_0 \tag{36}$$

denotes the surface density of monomers. Here, a_0 is the so-called jump distance, E is the kinetic barrier of nucleation, n_0 denotes the mean number of monomers per unit volume and the remaining quantities have their obvious meanings. Taking $a_0 \approx n_0^{-1/3}$

and $n_0 \approx N_A/V_M$, one gets for ω

$$\omega = \left(\frac{kT}{h}\right)\left(\frac{N_A}{V_M}\right)^{2/3} \exp\left(-\frac{E}{kT}\right) \tag{37}$$

In most cases, the unknown quantity E is frequently approximated by the activation energy of diffusion. Or, application of the Stokes–Einstein relation between diffusion and viscosity η leads to [19]

$$\omega = \frac{kT}{3\pi\eta}\left(\frac{N_A}{V_M}\right)^{5/3} \tag{38}$$

Again, the detachment frequency $k^-(n)$ can be determined from relationship (28). Some typical values of the above quantities for the silicate glass $Li_2O{\cdot}2SiO_2$ are collected in Table 1. For this system, the temperature dependence of the viscosity was

Table 1
Material parameters for $Li_2O{\cdot}2SiO_2$

Symbol	Parameter	Value
T_E	Melting temperature	1313 K
V_m	Molar volume	$6.11 \times 10^{-5}\,m^3\,mol^{-1}$
Δh	Heat of fusion	$5.4 \times 10^4\,J\,mol^{-1}$
σ	Interfacial energy	$0.150\,J\,m^{-2}$

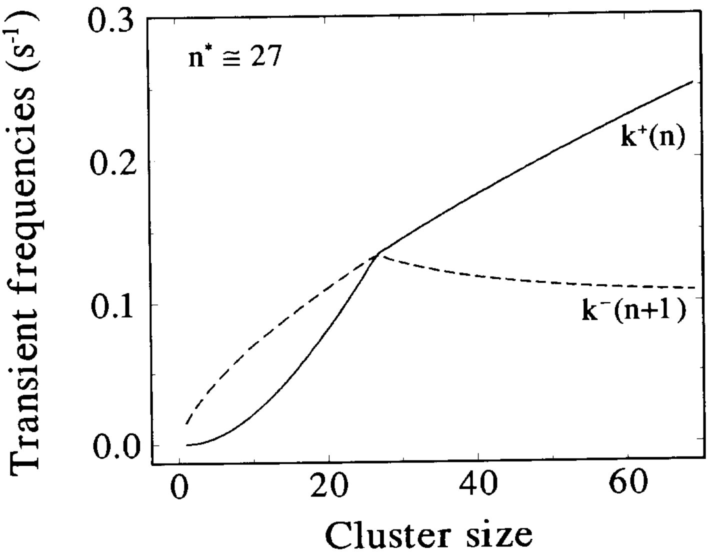

Fig. 3. Transient probabilities $k^{\pm}(n)$ as a function of cluster size at 800 K for lithium disilicate glass.

taken as [19]

$$\eta = 0.363\exp\left(\frac{7759.7}{T-460}\right)(\mathrm{N\,s\,m^{-2}}) \tag{39}$$

A typical dependence of transient probabilities $k^{\pm}$ on cluster size is given in Fig. 3.

For the binary system, we have [14]

$$k_i^+(n_A, n_B) = b_i \exp\left(-\frac{E_i^+}{kT}\right), \quad i = \mathrm{A, B} \tag{40}$$

where

$$b_i = S(n_A, n_B)\left(\frac{N_A}{V_M}\right)^{2/3}\left(\frac{kT}{h}\right)X_i^L, \quad i = \mathrm{A, B} \tag{41}$$

Above, X_i^L is the initial molar fraction ("concentration") of the ith component in the liquid phase (it is usually assumed to be a constant during the nucleation process). The activation energies $E_{A,B}^+$ are given by

$$E_i^+ = E_i + \frac{1}{2}[1 + \mathrm{sign}\,\Delta g_i(n_A, n_B)]\Delta g_i(n_A, n_B), \quad i = \mathrm{A, B} \tag{42}$$

where

$$\Delta g_A(n_A, n_B) = \Delta G(n_A + 1, n_B) - \Delta G(n_A, n_B) \tag{43}$$

$$\Delta g_B(n_A, n_B) = \Delta G(n_A, n_B + 1) - \Delta G(n_A, n_B) \tag{44}$$

and the Gibbs free energies ΔG are expressed in Eq. (12), and the detachment frequencies k_i^- are given by conditions (29, 30). The energies $E_{A,B}$ can be identified with the activation energies of transition of an A (or B) particle across the phase interface. Here, we have chosen the following parameterization

$$\varepsilon = \frac{1}{2}(E_A + E_B) \tag{45}$$

$$r = \exp\left(\frac{E_A - E_B}{kT}\right) \tag{46}$$

where r is the so-called kinetic parameter. Introduced in such a way, the kinetic parameter coincides with Stauffer's definition: $r = k_B^+/k_A^+$ [20] for $X_B^L = 0.5$ near the saddle point when $\Delta g_i(n_A, n_B) = 0$.

3.3. Nucleation equations

In order to derive an equation expressing the evolution of a nucleation process, some simplifications are used. The basic assumptions of nucleation theory are the following [21]

(i) A nucleation process has no memory, i.e. the present state of a nucleating system does not depend on its previous evolution stages. In other words, the process is a Markovian one;

(ii) Coalescence (Oswald ripening) of the large clusters is neglected;
(iii) Mutual interactions of the clusters are also neglected. This means that the system clusters + parent phase (however non-ideal) is assumed to be an ideal solution.

Under these assumptions, the equation describing the nucleation process, in a single-component system, reads

$$\frac{\mathrm{d}F(n,t)}{\mathrm{d}t} = J(n-1,t) - J(n,t) \tag{47}$$

where

$$J(n,t) = k^{+}(n,t)F(n,t) - k^{-}(n+1,t)F(n+1,t) \tag{48}$$

defines the cluster flux density and $F(n,t)$ represents the fundamental quantity of nucleation theory, the distribution function of the clusters, i.e. the number of newly-formed clusters of size n in unit volume at time t. In continuous cluster-size space n, i.e. in the case when n is sufficiently large, and using detailed balance conditions, the nucleation equation can be rewritten to be

$$\frac{\partial F(n,t)}{\partial t} + \frac{\partial J(n,t)}{\partial n} = 0 \tag{49}$$

where

$$J(n,t) = -k^{+}(n,t)F_0(n)\frac{\partial}{\partial n}\left[\frac{F(n,t)}{F_0(n)}\right] \tag{50}$$

Here, $F_0(n)$ is the equilibrium distribution function, defined by relationship (31).

For nucleation in a binary system, the above Zeldovich–Frenkel equation takes the form

$$\frac{\mathrm{d}F(n_\mathrm{A},n_\mathrm{B},t)}{\mathrm{d}t} = J_\mathrm{A}(n_\mathrm{A}-1,n_\mathrm{B},t) - J_\mathrm{A}(n_\mathrm{A},n_\mathrm{B},t) + J_\mathrm{B}(n_\mathrm{A},n_\mathrm{B}-1,t) - J_\mathrm{B}(n_\mathrm{A},n_\mathrm{B},t) \tag{51}$$

with the fluxes

$$J_\mathrm{A}(n_\mathrm{A},n_\mathrm{B},t) = k_\mathrm{A}^{+}(n_\mathrm{A},n_\mathrm{B})F(n_\mathrm{A},n_\mathrm{B},t) - k_\mathrm{A}^{-}(n_\mathrm{A}+1,n_\mathrm{B})F(n_\mathrm{A}+1,n_\mathrm{B},t) \tag{52}$$

$$J_\mathrm{B}(n_\mathrm{A},n_\mathrm{B},t) = k_\mathrm{B}^{+}(n_\mathrm{A},n_\mathrm{B})F(n_\mathrm{A},n_\mathrm{B},t) - k_\mathrm{B}^{-}(n_\mathrm{A},n_\mathrm{B}+1)F(n_\mathrm{A},n_\mathrm{B}+1,t) \tag{53}$$

and where the distribution function $F(n_\mathrm{A},n_\mathrm{B},t)$ represents the number of clusters consisting of n_A and n_B particles at time t in unit volume of the parent phase. Similarly as before, at the continuous level of description the above equation transforms to

$$\frac{\partial F(n_\mathrm{A},n_\mathrm{B},t)}{\partial t} + \frac{\partial J_\mathrm{A}(n_\mathrm{A},n_\mathrm{B},t)}{\partial n_\mathrm{A}} + \frac{\partial J_\mathrm{B}(n_\mathrm{A},n_\mathrm{B},t)}{\partial n_\mathrm{B}} = 0 \tag{54}$$

where the appropriate cluster flux densities are defined as

$$J_i(n_\mathrm{A},n_\mathrm{B},t) = -k_i^{+}(n_\mathrm{A},n_\mathrm{B},t)F_0(n_\mathrm{A},n_\mathrm{B})\frac{\partial}{\partial n_i}\left[\frac{F(n_\mathrm{A},n_\mathrm{B},t)}{F_0(n_\mathrm{A},n_\mathrm{B})}\right], \quad i = \mathrm{A},\mathrm{B} \tag{55}$$

with the equilibrium distribution F_0 given by Eq. (32) and k_i^{+} by Eqs. (26) and (40).

In order to solve the aforementioned nucleation equations, the initial, and boundary, conditions have to be introduced. Usually, it is assumed that the nucleation process starts from the monomers (single atoms or molecules of parent phase) and that no other clusters are present within the metastable vapor or liquid. Moreover, the number of monomers equals the equilibrium distribution function F_0. The second boundary condition reflects the assumption that the distribution function of newly-forming clusters remains finite as $n \rightarrow \infty$. (In other words, the formation of extremely large nuclei is excluded.) Consequently, the initial and boundary conditions read

$$F(n, t \rightarrow 0) = F_0(n) \quad \text{for } n \leq 1 \tag{56}$$

$$\left. \frac{F(n,t)}{F_0(n)} \right|_{n \rightarrow 1} = 1 \tag{57}$$

$$F(n \rightarrow \infty, t) = 0 \tag{58}$$

For the binary system we have

$$F(n_A, n_B, t \rightarrow 0) = F_0(n_A, n_B) \quad \text{for } n_A + n_B = 1 \tag{59}$$

$$F(n_A, n_B, t \rightarrow 0) = 0, \quad \text{under other conditions} \tag{60}$$

$$F(n_A, n_B, t) = 0 \quad \text{for } n_A + n_B \rightarrow \infty \tag{61}$$

From the distribution function, many important characteristics of nucleation processes may be determined. Most "popular" in engineering applications seem to be the so-called nucleation rate I and the integrated cluster flux Z. At constant temperature (or at constant supersaturation), the former corresponds simply to the cluster flux density taken at critical cluster size and can readily be calculated from Eq. (50)

$$I(t) = J(n^*, t) = -k^+(n^*) F_0(n^*) \left[\frac{\partial}{\partial n} \frac{F(n,t)}{F_0(n)} \right]_{n^*} \tag{62}$$

In general (at variable supersaturations or temperatures), $I(t)$ represents the number of supercritical clusters per unit volume, which can be expressed as [22]

$$I(t) = J(n^*, t) - \frac{\mathrm{d}n^*}{\mathrm{d}t} F(n^*, t) \tag{63}$$

The latter, directly measurable quantity is connected with the total number of supercritical clusters appearing within the original phase during the time of observation t

$$Z(t) = \int_0^t J(n^*, \tau) \mathrm{d}\tau = \sum_{n > n^*} F(n, t) \tag{64}$$

Similar relationships can also be derived for binary systems.

Nucleation equations, together with the initial and boundary conditions, completely define the problem of homogeneous nucleation at the kinetic level. To solve them either proper numerical methods have to be used or an approximate analytical solution could be found. We shall not specify in detail the methods of solution—readers more interested in the mathematics can find more information elsewhere, e.g. in Refs. [17, 23, 24]. Below, some applications are summarized.

4. Results

In this Section, we have collected some interesting results following from our previous studies of transient nucleation in single-component and binary systems occurring under constant, and variable, temperature regimes. In the case of a single-component system we compare our analytical formulae, obtained by our novel method based on the boundary layer theory combined with Green's function technique [17], with our exact numerical simulations and also with the available experimental data [25] related to the glassy system $Li_2O{\cdot}2SiO_2$ (see also Table 1 for parameters used). However, due to a lack of suitable data, the binary system used in our computations is represented by fictitious model material.

4.1. Nucleation at constant temperature

4.1.1. Single-component system

Applying our analytical method [17] to obtain approximate analytical solution of nucleation equation (49), one gets for a normalized distribution function

$$y(n,\vartheta) = \frac{F(n,\vartheta)}{F_0(n)} = \frac{1}{2}\operatorname{erfc}(K_1\sqrt[3]{n} + K_2) \tag{65}$$

where erfc denotes the so-called complementary error function, and

$$K_1 = \frac{3(n^*)^{(-1/3)}}{\varepsilon}\frac{1}{\sqrt{1-\exp(-2\vartheta)}} \tag{66}$$

$$K_2 = \frac{3(1-(n^*)^{(-1/3)})\exp(-\vartheta)-1}{\varepsilon\sqrt{1-\exp(-2\vartheta)}} \tag{67}$$

Above, ε is a small parameter containing basic information about thermodynamical properties (via $\Delta\mu, \sigma, T$) of the system under consideration, and $\vartheta = t/\tau$ is the time normalized by a quantity τ, which is closely connected with the transition frequencies. (For more details, see Refs. [17] and [23].) The dependence of the normalized distribution function both on the cluster size n and on ϑ is shown in Fig. 4.

In terms of distribution function, other important characteristics of a nucleation process may be derived. Actually, according to definition (62), the nucleation rate may be readily determined to be

$$I(\vartheta) = J(n^*,\vartheta) = \frac{J^S(n^*)}{\sqrt{1-\exp(-2\vartheta)}}\exp\left\{-\left[\frac{3(1-(n^*)^{(-1/3)})\exp(-\vartheta)}{\varepsilon\sqrt{1-\exp(-2\vartheta)}}\right]^2\right\} \tag{68}$$

where $J^S(n^*)$ corresponds to its stationary value. In Fig. 5, the nucleation rates (normalized to J^S) obtained by various authors are compared with our numerical calculations and also with our formula (68).

Using definition (64), another interesting and directly measurable quantity of the transient nucleation process can be derived: the so-called integrated flux. In Fig. 6, the analytical and numerical computations of this quantity are compared with experimen-

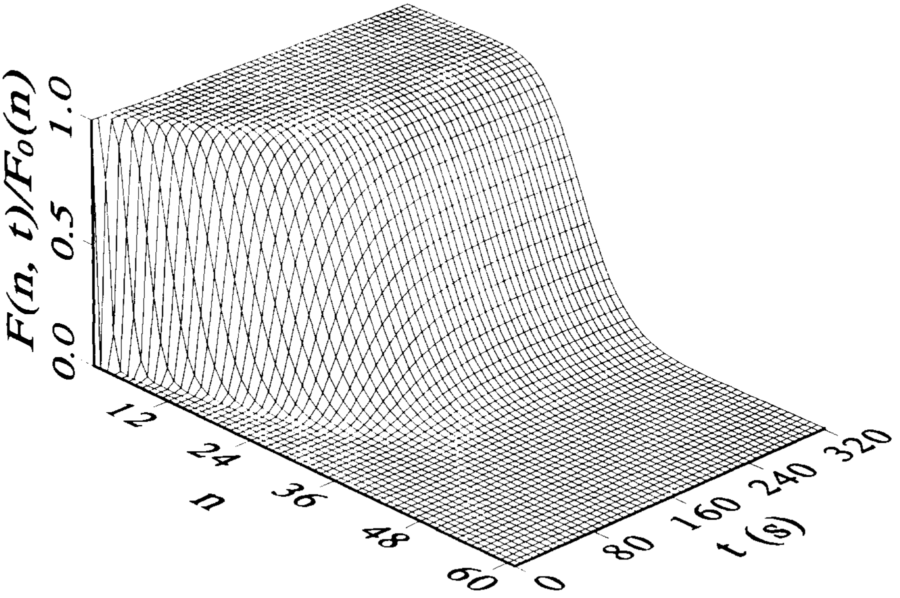

Fig. 4. Qualitative dependence of the dimensionless distribution function $y(n,t) = F(n,t)/F_0(n)$ on cluster size n and time t.

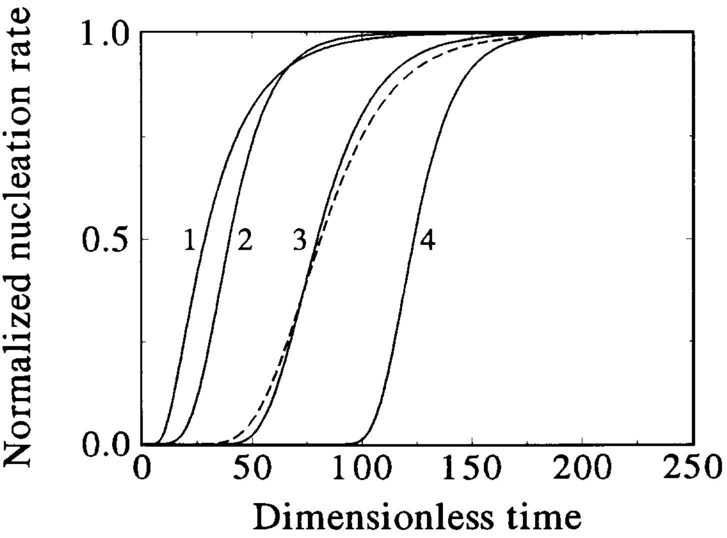

Fig. 5. Normalized nucleation rate as a function of dimensionless time: 1, Kashchiev [26]; 2, Shi et al. [27]; 3, relationship (68); 4, Trinkaus and Yoo [21]; – – –, numerical simulation ($T = 800$ K, $n^* \approx 27$).

tal data [25]. From this dependence, the so-called time lag, i.e. the time corresponding to the moment at which the addition of the supercritical clusters (nuclei) within the metastable parent phase becomes linear with the time, can be deduced. (In other words, the steady-state is reached by the nucleating system.) It can be felt intuitively that the integrated flux depends on the thermodynamic and kinetic properties of the system. Indeed, such a dependence is depicted in Fig. 7, where the sensitivity of the time lag on the surface tension between a nucleus and its ambient phase is shown. It can also be seen that our analytical results are in much better agreement with exact numerical calculations than other previous approaches [21, 28].

4.1.2. *Binary system*

For the case of nucleation of two-component (A, B) systems, we have (with respect to the single-component system) an additional parameter, the mole fraction of the B component. Reiss [12] suggested the kinetic equations describing binary nucleation process and applied this model for stationary homogeneous nucleation in a binary mixture. From that time, various analytical approaches [20, 29–31] to the stationary nucleation rate appeared, based on the restriction that the nucleation rate is controlled by the flow of nuclei through the saddle point. Recently, several works [14, 28, 32, 33] have shown that such an approximation is not generally acceptable.

Here, let us briefly summarize the main results of transient binary nucleation. As in our previous works [14, 34], we have used the following values of the parameters: $V_M = 6.11 \times 10^{-5}\,\mathrm{m^3\,mol^{-1}}$, $\Delta h_A^0 = 5 \times 10^4\,\mathrm{J\,mol^{-1}}$, $\Delta h_B^0 = 6 \times 10^4\,\mathrm{J\,mol^{-1}}$, $T_A^0 = 1300\,\mathrm{K}$, $T_B^0 = 1250\,\mathrm{K}$ and $\sigma = 0.150\,\mathrm{J\,m^{-2}}$, for model ideal solution.

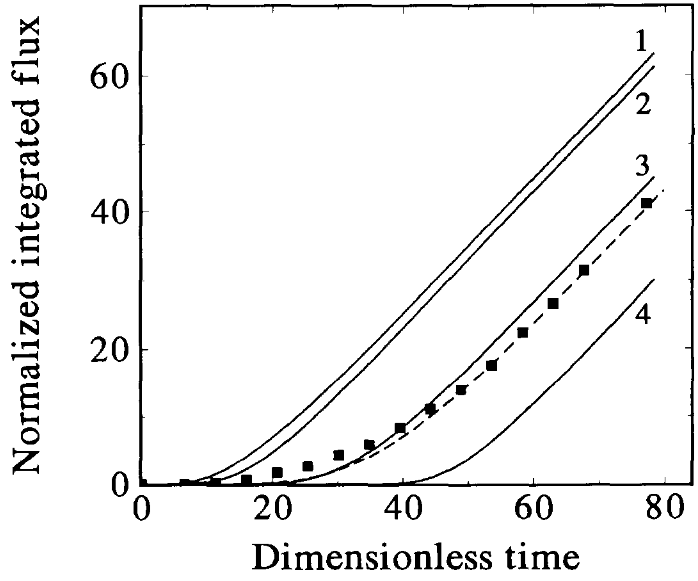

Fig. 6. Number of nuclei (normalized integrated flux) as a function of dimensionless time: 1, Kashchiev [26]; 2, Shi et al. [27]; 3, our solution [17]; 4, Trinkaus and Yoo [21]; – – –, numerical computation; ■, experimental data [25].

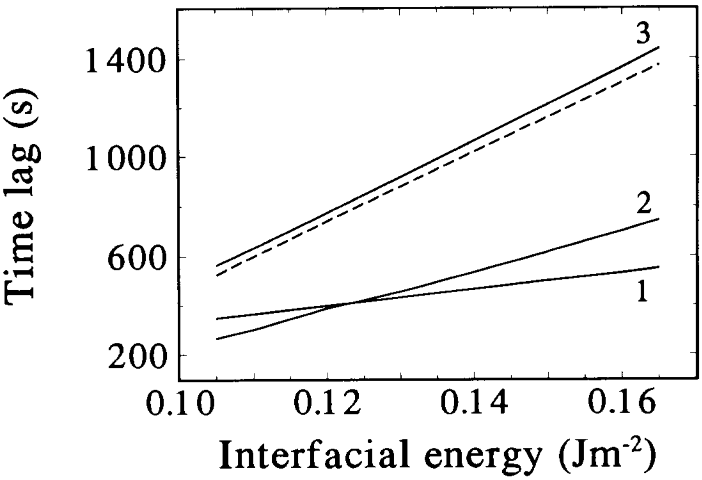

Fig. 7. Time lag as a function of interfacial energy: 1, Kashchiev [26]; 2, Shi et al. [27]; 3, our solution [24]; – – –, numerical simulation at $T = 800$ K and $E = 4.075 \times 10^{-19}$ J m^{-2}.

The nucleation rate $J(n, \vartheta)$ corresponds to the sum of $(J_A + J_B)$ over the cluster composition (see Ref. [14]). In such a sense, this is analogous to the nucleation rate of a single-component system. With a sufficiently long time for various cluster sizes $n = 20$ (full lines) and 30 (dashed lines) molecules, $J(n, \vartheta)$ reaches some stationary value $J^S = J(n, \vartheta \rightarrow \infty)$, which depends on the temperature, see Fig. 8. Clusters of $n = 20$ molecules at $T = 790$ K have a subcritical value ($n^* \approx 28$ molecules) and reach

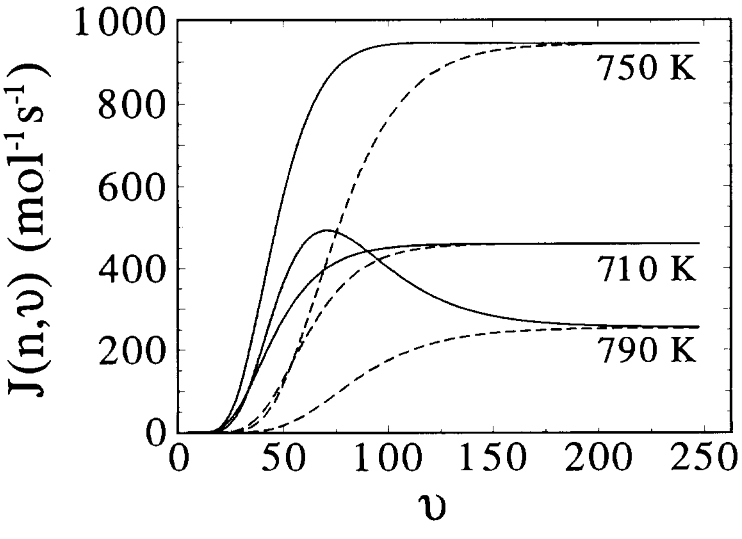

Fig. 8. Nucleation rate J as a function of dimensionless time ϑ for cluster size $n = 20$ (—) and 30 (– – –) molecules at $T = 750$, 710 and 790 K for mole fraction of solution $X_B^L = 0.5$.

some extremum value, as does the cluster flux for subcritical size in single-component system.

The mean cluster composition at the stationary limits ($\vartheta = 250$ seems to be a sufficiently long time for reaching a stationary value) goes to the mole fraction of the saddle point $C_S = n_B^*/(n_A^* + n_B^*)$ only for sufficiently small sizes ($n \leq (n_A^* + n_B^*)/2$) at various temperatures (see Fig. 9). Certainly, the critical size n^* increases with the temperature, which corresponds to the mean cluster composition behaviour (for details, see Ref. [34]).

The temperature dependence of the time lag for $n = 20$ (full line) and 40 (dashed line) molecules, together with the stationary nucleation rate (see Fig. 10) for $X_B^L = 0.5$, is qualitatively the same as in a single-component system. J^S reaches some extremum value near $T = 745$ K.

The stationary nucleation rate J^S increases and the differences between time lags of various sizes ($n = 20, 25, 30$ and 35 molecules) decreases with increasing X_B^L (see Fig. 11). This is caused by the fact that critical size decreases with X_B^L and implies an increase in nucleation rate (for the chosen data). At the same time, the growth rate of supercritical nuclei increases with their size, which corresponds to shorter times of time lags of various sizes for increasing X_B^L. Increase in J^S with X_B^L is given predominantly by the values of Δh_A^0 and Δh_B^0, because the swapping of Δh_A^0 with Δh_B^0 leads to a decrease in J^S with X_B^L (for details, see Ref. [34]).

Time lags for cluster sizes $n = 20, 30$ and 40 molecules as a function of $\log_{10} r$ reach some minimal value near $\log_{10} r \approx 0.2$ (see Fig. 12a), but the differences in time lags for

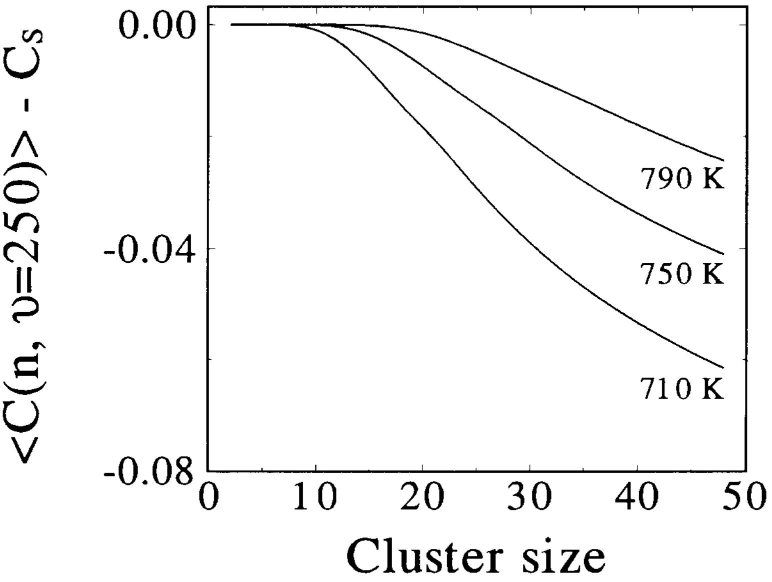

Fig. 9. Difference of mean cluster composition $\langle C(n, \vartheta) \rangle$ from mole fraction of the saddle point C_S at dimensionless time $\vartheta = 250$ as a function of cluster size for mole fraction of solution $X_B^L = 0.5$ at $T = 710$, 750 and 790 K.

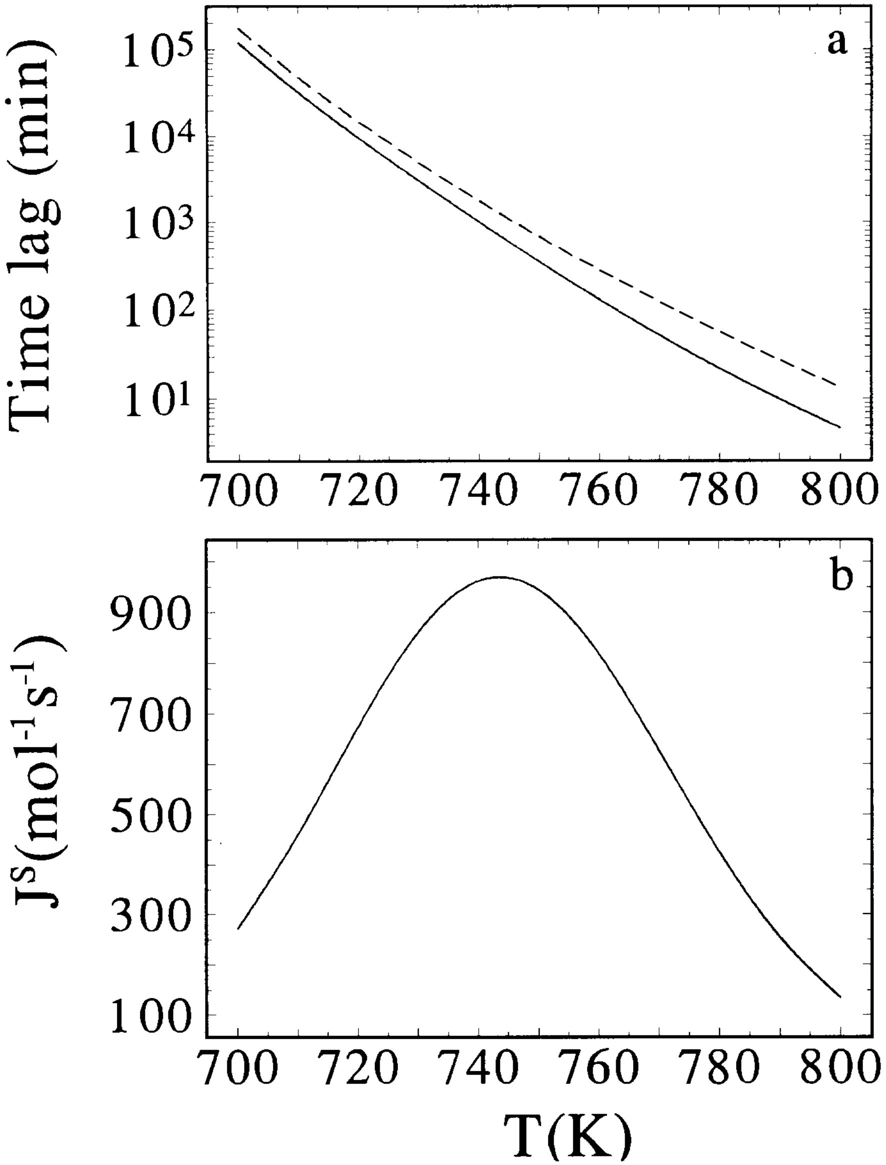

Fig. 10. a. Time lag for $n = 20$ (—) and 40 (– – –) molecules. b. Stationary nucleation rate J^S as a function of temperature T for $X_B^L = 0.5$.

various cluster sizes remain approximately constant. However, the nucleation rate increases with the kinetic parameters (see Fig. 12b), which can be explained by the fact that with increasing kinetic parameter r, k_B^+ increases (relative to k_A^+) and the B component is more supersaturated than A ($\Delta h_B^0 > \Delta h_A^0$ for the chosen data), which probably leads to an increase in J^S with kinetic parameter r.

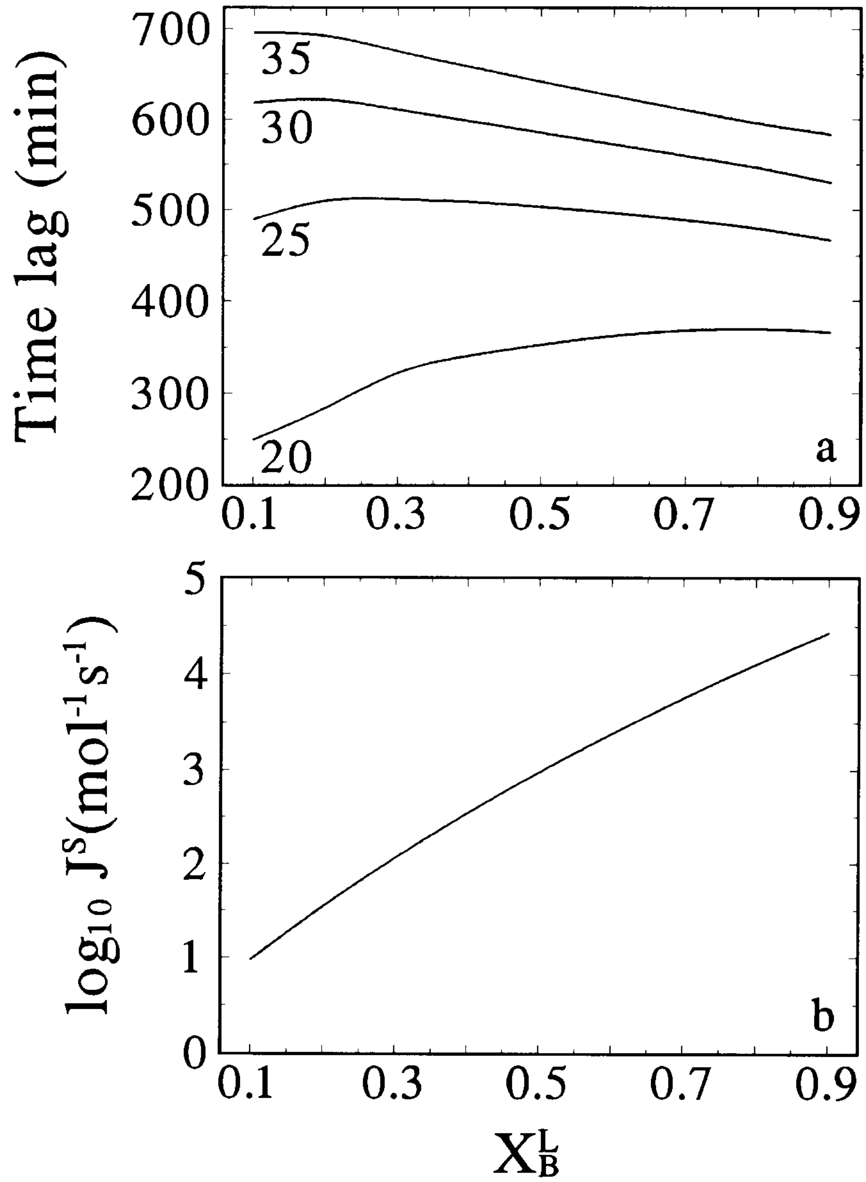

Fig. 11. a. Time lag for cluster sizes $n = 20, 25, 30$ and 35 molecules. b. Decimal logarithm of stationary nucleation rate J^S at $T = 750$ K as a function of mole fraction of solution X_B^L.

4.2. *Nucleation under various temperature regimes*

In the previous section, we considered nucleation at constant temperature. Now, let us consider nucleation under various temperature regimes, assuming that the kinetics of nucleation plays a dominant role, i.e. temperature changes within the system are

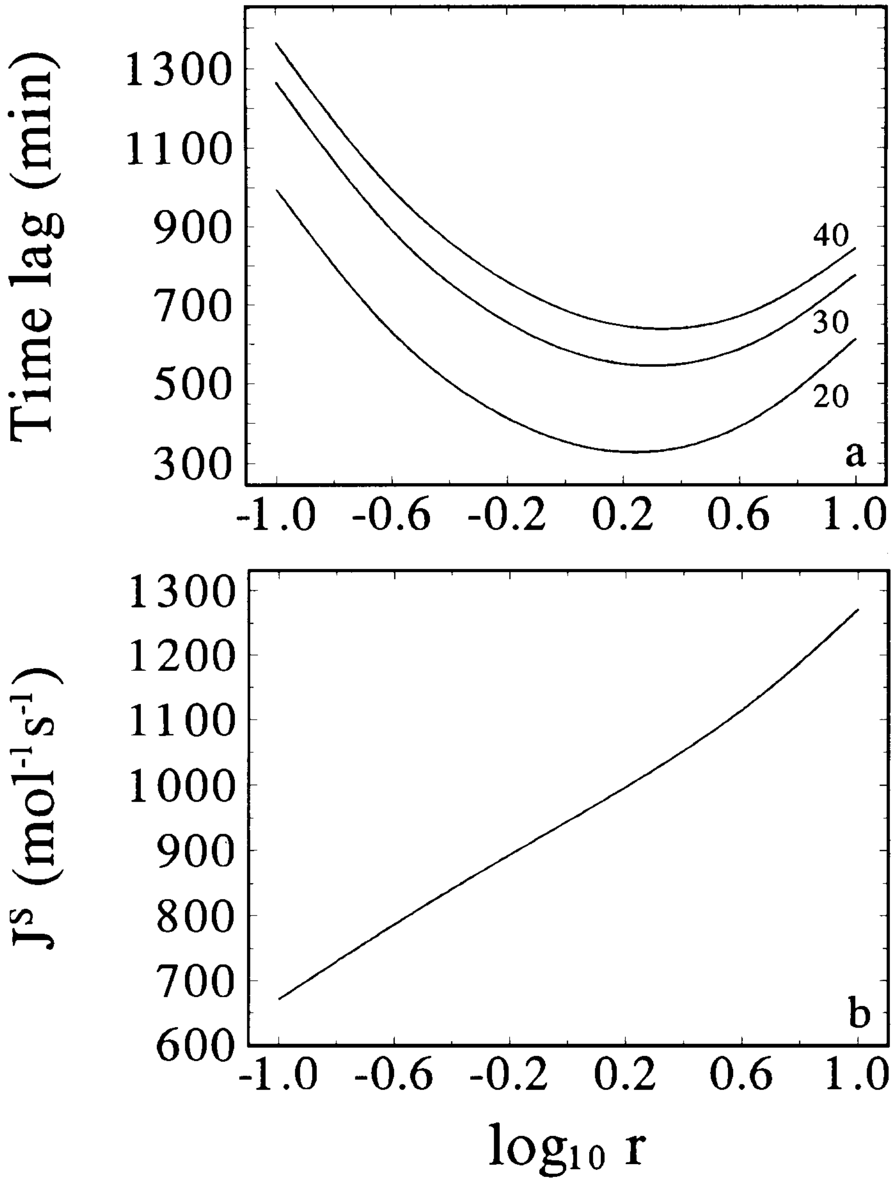

Fig. 12. a. Time lag for cluster sizes $n = 20, 30$ and 40 molecules. b. Stationary nucleation rate J^S as a function of decimal logarithm of kinetic parameter r at 750 K for $X_B^L = 0.5$.

faster than nucleation kinetics. In such a case, Eqs. (47) and (49) again hold, but the transient frequencies $k_{A,B}^{\pm}$ implicitly depend on time (through the temperature).

The simplest case (interesting from a technological point of view) is so-called two-step nucleation, when the effect of preliminary heat treatment on the kinetics of nucleation were modeled [35] and the results compared with measured data of nuclei for two-step annealing treatments in an $Li_2O{\cdot}2SiO_2$ melt.

The effect of the preliminary heat treatment at the temperature T_1 during time t_0 on the nucleation taking place at the different temperature T_2 can be considered as nucleation at the constant temperature T_1 followed by nucleation at the constant temperature T_2, because the temperature change $T_1(t_0) \rightarrow T_2$ is relatively fast with respect to the transient time of nucleation. Nucleation at the temperature T_2 starts naturally with the distribution function corresponding to the temperature T_1 at time t_0 (for details, see Ref. [35]).

First of all, we have chosen the interfacial energy σ and the activation energy of diffusion across the phase interface to get the best coincidence with known experimental data for the number of nuclei at constant temperature. The effect of "development" of nuclei, i.e. their further growth at development temperature to a size detectable in a microscope, was considered to obtain correct values of the σ and E parameters. Then, the number of nuclei for the critical size $n^* = 51$ at the development temperature were computed by numerical solution of the kinetic equation (47), without any fitting of σ and E parameters, and compared with experimental measurement of Fokin and co-workers [25, 36, 37], see Fig. 13. Here, nucleation (as for measured data) at temperature T_1 was considered as a preliminary heat treatment, i.e. time starts from t_0. We have obtained very good coincidence between the computed and measured number of nuclei, within experimental error, under various experimental conditions. The whole nucleation process (from the moment when temperature annealing at T_1 occurs) for critical size $n^* = 51$ at the development temperature, is depicted in Fig. 14. The cluster flux J_{51} jumps to the higher value at time t_0 and then relaxes to its stationary value at constant temperature T_2. A small increase in nucleation rate (1–2 orders in magnitude) after preliminary heat treatment at $T_1 < T_2$ is a known experimental fact [25], but which, however, is barely understandable. Recently it was shown (for details, see

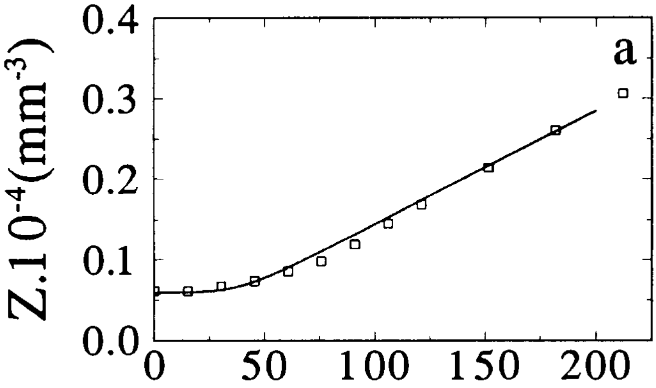

Fig. 13. Number of nuclei from Eq. (64) (—) and experimental number of nuclei Z as a function of time t at 738 K: (a) after annealing 758 K during $t_0 = 143$ min (□); at 758 K (b) after preliminary annealing at 713 K during $t_0 = 18$ h (□), 742 K during $t_0 = 4.5$ h (○) and 746 K during $t_0 = 45$ min (+); and at 713 K (c) after annealing at 738 K during $t_0 = 50$ min (□).

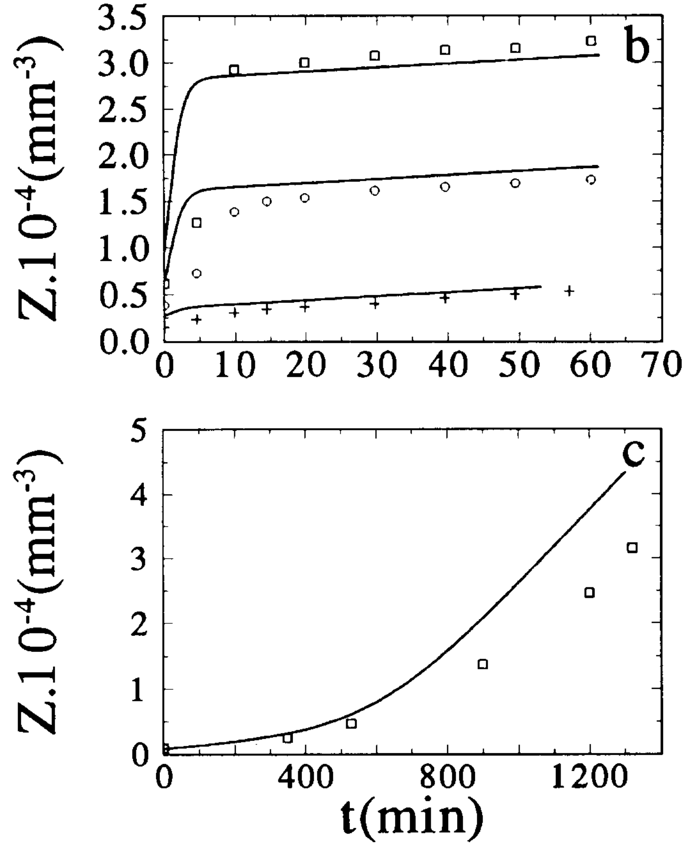

Fig. 13. (*Continued*)

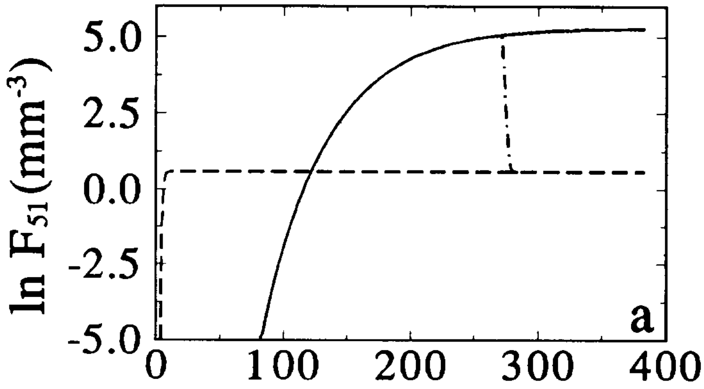

Fig. 14. The cluster distribution function F_{51} (a), the cluster current J_{51} (b) and the number of nuclei Z_{51} (c) as a function of time t at the constant temperature 724 K (—) and 758 K (– – –) and at 724 K ($t_0 = 4.5$ h) → 758 K (–·–·–).

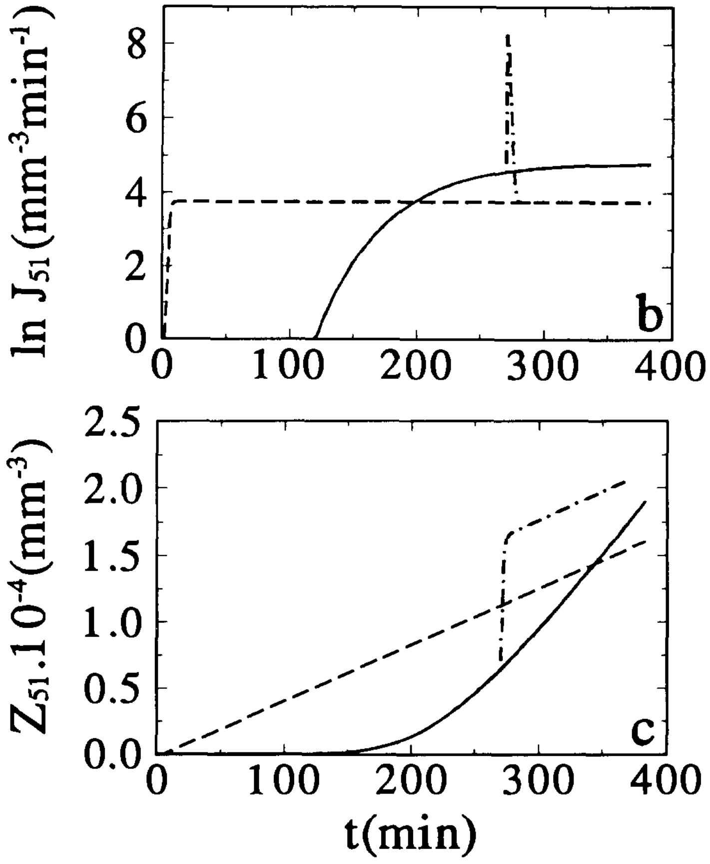

Fig. 14. (*Continued*)

Ref. [35]) that the increase in nucleation rate after the preliminary heat treatment is caused by an increase in the transient frequencies at the temperature change.

Furthermore, we have studied nucleation under various temperature regimes: linear cooling and heating [22], and oscillating temperature [18]. During heating (analogically for cooling), the nucleation rate at some temperature T can reach even higher values than that corresponding to its stationary value (for details, see Ref. [18]). This situation occurs when the stationary nucleation rate decreases with temperature, i.e. the nucleation rate is delayed, its value corresponding to lower tempeatures.

Temperature oscillations produce oscillations of the cluster distribution function, nucleation rate and the flux, in such a way that the amplitudes of these quantities grow with increasing temperature amplitude. Moreover, the amplitude of nucleation rate oscillations increases with the frequency of temperature oscillations which is predominantly influenced by the temporal change in the critical size (for details, see Ref. [18]).

5. Conclusion

We have presented some of the most important (and, we believe, most interesting) results on transient nucleation processes taking place in single and binary systems. Applying the described treatment of the problem, some important characteristics of nucleating systems may be determined, including the number of growable clusters (nuclei) per unit volume of mother phase, or the time required for their appearance. Knowledge of these quantities allows the nucleation process itself to be influenced from the outside.

It has to be pointed out, however, that the above model and methodology may be applied not only in the study of nucleation in traditional technological systems (crystals), but also in such exotic problems as the crystallization of viruses, nucleation in neutron stellar cores or in metastable nuclear matter. Analysis of these problems lies beyond the scope of this paper.

References

[1] F.F. Abraham, Homogeneous Nucleation Theory, Suppl. I, Advances in Theoretical Chemistry, Academic Press, New York and London, 1974.
[2] A.C. Zettlemoyer (Ed.), Nucleation Phenomena, Elsevier, Amsterdam, 1977.
[3] B. Mutaftschiev, Crystal Growth in Science and Technology, NATO Advanced Study Institute, Erice, Italy, 1987.
[4] D.W. Oxtoby, J. Phys.: Condens. Matt., 4 (1992) 7627.
[5] A. Milchev, Contemp. Phys., 32 (1991) 321.
[6] W. Kurz and D.J. Fisher, Fundamentals of Solidification, Trans. Tech. Publ., Switzerland, 1984.
[7] C.V. Thompson and F. Spaepen, Acta Metall., 27 (1979) 1855.
[8] I. Penkov and I. Gutzow, J. Mater. Sci., 19 (1984) 233.
[9] K. Takahashi and T. Yoshio, Yogyo-Kyokai-Shi, 81 (1973) 524.
[10] J. Šesták, Thermochim. Acta, 95 (1985) 459.
[11] T. Kemény and J. Šesták, Thermochim. Acta, 110 (1987) 113.
[12] H. Reiss, J. Chem. Phys., 18 (1950) 840.
[13] A.L. Greer, P.V. Evans, R.G. Hamerton and D.K. Shangguan, J. Cryst. Growth, 99 (1990) 38.
[14] Z. Kožíšek and P. Demo, J. Cryst. Growth, 132 (1993) 491.
[15] P. Harrowell and D.W. Oxtoby, J. Chem. Phys., 80 (1984) 1639.
[16] J.E. Mayer and M.G. Mayer, Statistical Mechanics, Wiley Interscience, New York, 1977.
[17] P. Demo and Z. Kožíšek, Phys. Rev., B48 (1993) 3620.
[18] Z. Kožíšek and P. Demo, J. Non-Cryst. Solids, 152 (1993) 201.
[19] E.G. Rowlands and P.F. James, Phys. Chem. Glass, 20 (1979) 1.
[20] D. Stauffer, J. Aerosol. Sci., 7 (1976) 319.
[21] H. Trinkaus and M.H. Yoo, Philos. Mag., A55 (1987) 269.
[22] Z. Kožíšek and Z. Chvoj, in Z. Chvoj, J. Šesták and A. Tříska (Eds.), Kinetic Phase Diagrams, Elsevier, Amsterdam, 1991, p. 277.
[23] P. Demo and Z. Kožíšek, Mater. Sci. Eng., A173 (1993) 41.
[24] P. Demo and Z. Kožíšek, Philos. Mag., B70 (1994) 49.
[25] V.M. Fokin, A.M. Kalinina and V.N. Filipovich, J. Cryst. Growth, 52 (1981) 115.
[26] D. Kashchiev, Surf. Sci., 14 (1969) 209.
[27] G. Shi, J.H. Seinfeld and K. Okuyama, Phys. Rev., A41 (1990) 2101.
[28] G. Shi and J.H. Seinfeld, J. Chem. Phys., 93 (1990) 9033.
[29] J.O. Herschfelder, J. Chem. Phys., 62 (1975) 3763.

[30] C.S. Kiang, R.D. Cadle, P. Hamil, V.A. Mohnen and G.K. Yue, J. Aerosol. Sci., 6 (1975) 465.
[31] K. Binder and D. Stauffer, Adv. Phys., 25 (1976) 343.
[32] H. Vehkamäki, P. Paatero, M. Kulmala and A. Laaksonen, J. Chem. Phys., 101 (1994) 9997.
[33] D.E. Temkin and V.V. Shevelev, J. Cryst. Growth, 66 (1984) 380.
[34] Z. Kožíšek and P. Demo, Transient nucleation in binary ideal solution, J. Chem. Phys., 102 (1995), in press.
[35] Z. Kožíšek and P. Demo, J. Cryst. Growth, 147 (1995) 215.
[36] A.M. Kalinina, V.M. Fokin and V.N. Filipovich, Fiz. Khim. Stekla, 3 (1977) 122.
[37] V.M. Fokin, V.N. Filipovich and A.M. Kalinina, Fiz. Khim. Stekla, 3 (1977) 129.